Published in final edited form as:
Expert Rev Med Devices. 2012 November ; 9(6): 595–612. doi:10.1586/erd.12.58.

Coaxial electrospray of microparticles and nanoparticles for biomedical applications

Leilei Zhang[1,2,‡], **Jiwei Huang**[1,3,‡], **Ting Si**[4,‡], and **Ronald X Xu**[1,2,3,*]

[1]Department of Biomedical Engineering, The Ohio State University, Columbus, OH 43210, USA

[2]Department of Ophthalmology, The Ohio State University, Columbus, OH 43210, USA

[3]Biophysics Graduate Program, The Ohio State University, Columbus, OH 43210, USA

[4]Department of Modern Mechanics, University of Science and Technology of China, Hefei 230027, China

Abstract

Coaxial electrospray is an electrohydrodynamic process that produces multilayer microparticles and nanoparticles by introducing coaxial electrified jets. In comparison with other microencapsulation/nanoencapsulation processes, coaxial electrospray has several potential advantages such as high encapsulation efficiency, effective protection of bioactivity and uniform size distribution. However, process control in coaxial electrospray is challenged by the multiphysical nature of the process and the complex interplay of multiple design, process and material parameters. This paper reviews the previous works and the recent advances in design, modeling and control of a coaxial electrospray process. The review intends to provide general guidance for coaxial electrospray and stimulate further research and development interests in this promising microencapsulation/nanoencapsulation process.

Keywords

coaxial electrospray; drug delivery; electrohydrodynamic atomization; instability analysis; microparticle; multimodal imaging; nanoparticle; scaling law; Taylor cone

Polymeric microparticles (MPs) and nanoparticles (NPs) have been widely explored as biodegradable carriers for controlled delivery and sustained release of various therapeutic agents, such as drugs, proteins and genes [1–4]. MPs and NPs can be conjugated with antibodies, peptides and other disease-targeting moieties for disease detection and therapy [5]. PEGylating these MPs and NPs will further reduce the immunogenicity and extend their circulation lifetime [6,7]. Encapsulating multiple imaging agents in MPs and NPs will facilitate multimodal contrast enhancement in various imaging modalities, such as

*Author for correspondence: Tel.: +1 614 688 3635, Fax: +1 614 292 7301, xu.202@osu.edu.
‡Three authors contributed equally to this article.

Financial & competing interests disclosure
The authors are grateful for the support of the following agencies: National Cancer Institute (grant no: R21CA15977 to RX Xu), Ohio Lion's Eye Research Foundation (Fellowship support to L Zhang), and Natural Science Foundation of China (Project No. 11002139 to T Si). The authors have no relevant affiliations or financial involvement with any organization or entity with a financial interest in or financial conflict with the subject matter or materials discussed in the manuscript. This includes employment, consultancies, honoraria, stock ownership or options, expert testimony, grants or patents received or pending, or royalties.
No writing assistance was utilized in the production of this manuscript.

ultrasonography, fluorescence imaging, photoacoustic imaging and MRI [8–11]. Loading both imaging and therapeutic agents in multi-functional MPs and NPs will enable image-guided therapy, image-guided drug delivery and other theranostic applications [12–14].

Drug-loaded MPs and NPs can be fabricated by many processes, such as emulsification, soft lithography, polymeric micelles, spray drying and microchannel extrusion [15,16]. Emulsification is the most commonly used method for microencapsulation/nanoencapsulation. A single emulsification process consists of consecutive steps of mixing two immiscible phases at a high speed, solidifying the drug-loaded particles and extracting the particles from the liquid phase [17,18]. A double emulsification process produces drug-loaded MPs and NPs following a four-step procedure [11,19]. First, an aqueous solution of payloads is emulsified in an organic solution of the carrier material to form water-in-oil (w/o) emulsion. Second, the first emulsion is emulsified in a large volume of water to form a water-in-oil-in-water (w/o/w) emulsion. Third, the organic solvent is evaporated or extracted to obtain particles with a solid shell. Finally, the particles are washed, centrifuged and lyophilized. Although emulsification is a relatively simple process to produce drug-loaded MPs and NPs, its encapsulation rate is low, especially for encapsulating water-soluble payloads. Besides, MPs and NPs fabricated by emulsification typically have a broad size distribution. Further, the application of mechanical forces and the addition of chemical reagents in an emulsification process may introduce protein denaturation and aggregation [20]. Considering the limitations of emulsification and other existing encapsulation processes, it is important to develop new methods for loading therapeutic and imaging agents in MPs and NPs with high productivity, high encapsulation efficiency, uniform size distribution and effective protection of bioactivity.

Coaxial electrospray is an emerging technology with the potential to overcome the above limitations. Also known as coaxial electrohydrodynamic atomization, this process produces multilayer particles with size ranging from tens of nanometers to hundreds of micrometers by introducing an elevated electric field between a coaxial capillary needle and ground [21–24]. The resultant electrical shear stress elongates the core and the shell liquid menisci at the needle outlet to form an inverted triangle shape called a ‘Taylor cone’. At the end of the Taylor cone, the jet of liquid extends from millimeters to centimeters and is broken into multilayer droplets owing to the electrohydrodynamic forces. This process has the potential to achieve high encapsulation rate (nearly 100%), precise control of the core-shell geometry, and protection of the fragile therapeutic cargos from process-induced denaturation and aggregation [21,23]. This is also a scalable process for mass production of drug-loaded MPs and NPs.

This paper reviews the previous works and the current advances in the field of coaxial electrospray. The paper starts with the history of the process, followed by discussions about important design variables, process parameters and material properties contributing to the process outcome. The mathematical analysis of the process and the characterization methods for the fabricated MPs and NPs are also reviewed. The paper concludes with the Key issues and a Five-year view of the technology.

History

Coaxial electrospray is a microencapsulation/nanoencapsulation process with a short history of 10 years. It was developed based on a traditional process of single-axial electrospray (also called ‘electrospray’ in general) that can be traced back to almost a century ago when Zeleny first studied the electrical discharge from liquid surfaces [25,26]. In 1960s, Taylor studied the disintegration of water drops in strong electric fields and observed the formation of Taylor cone [27]. Since then, electrospray has been studied extensively from both theoretical

and experimental points of view, with successful implementation in many applications such as mass spectrometry and tissue engineering. Considering that a number of publications are already available in the field of single-axial electrospray [28–32], this paper will not review electrospray in general, but focus on the niche area of coaxial electrospray. The technical transition from single-axial electrospray to coaxial electrospray was stimulated by the recent advances in nanotechnology and life science. Many efforts have been made in recent years to modify the traditional electrospray process in order to fabricate multi-functional MPs and NPs with improved quality and productivity. One example is the development of a liquid–liquid electrospray system to produce nano-silica particles [33,34]. Another example is the integration of the emulsion method with electrospray [11,35,36].

Coaxial electrospray modifies the single-axial electrospray process by using a coaxial capillary needle to deliver two liquids independently. Commonly used liquid materials for this process include water, glycerol, ethanol, ethylene glycol, lipid and olive oil. Multilayer MPs and NPs with hard shells can be fabricated using polymer materials, such as polymethylsilsesquioxane (PMSQ), poly(lactide-coglycolide) (PLGA), poly(lactide) (PLA), polystyrene, poly(methyl methacrylate) and polycaprolactone. In 2002 Loscertales *et al.* first fabricated monodisperse capsules with the diameter ranging from 0.15 to 10 μm by generating stable coaxial jets of two immiscible liquids [21]. Since then, many technical advances have been made for continuous improvement of this novel microencapsulation/nanoencapsulation process. Hwang *et al.* produced uniform-sized microcapsules with a polystyrene or poly(methyl methacrylate) core and a PCL shell by coaxial electrospray [37]. Farook *et al.* used a model glycerol–air system for co-axial electrohydrodynamic atomization of microbubble suspensions [22,38]. With a similar process setup, this group also fabricated microbubbles with various shells such as phospholipids, PLGA and PMSQ [22,24,38–43]. Xie *et al.* encapsulated bovine serum albumin (BSA) and lysozyme in a PLA shell by coaxial electrospray [23]. Xu *et al.* studied the morphological and structural properties of two-phase coaxial jet electrosprayed BSA–PLA capsules [44]. Nie *et al.* used coaxial electrospray to load paclitaxel and suramin in polymer microspheres for the treatment of brain tumors [45]. Lee *et al.* studied the release profile characteristics for biodegradable polymer-coated drug particles fabricated by coaxial electrospray [17]. Wu *et al.* integrated microfluidic method with coaxial electrospray to fabricate theranostic lipoplexes [46]. Park *et al.* combined the spray drying with coaxial electrospray to produce pH-responsive hydrogels [47]. Zhang *et al.* extended the application of coaxial electrospray to improve oral absorption of poorly water-soluable drug [48]. Lee *et al.*, Kim *et al.* and Ahmad *et al.* developed tri-needle coaxial electrospray systems to encapsulate multiple drugs in monodisperse polymer particles [17,49,50].

In addition to the above experimental advances, theoretical efforts have also been made for process modeling and optimization. Lopez-Herrera *et al.* implemented the scaling laws to study how the inner and outer flow rates affect the transported current by the coaxial jets and the size of the resultant droplets [51]. Marin *et al.* used the scaling laws to predict the inner and outer diameters of an electrified coaxial jet [52]. Mei *et al.* explored the relationship between the formation of core-shell structure and the ratio of charge relaxation lengths, as well as the ratio of inertial breakup lengths for inner and outer jets [53,54]. They concluded that the core-shell structured droplets could only be formed when the ratio of charge relaxation lengths and the ratio of inertial breakup lengths for inner and outer jets satisfied the specific requirements. Higuera introduced a quasi-unidirectional model of the coaxial flow and the transport of electric charge, which was an extension of the models used for single liquid jets [55]. The results were further compared with boundary element solutions of the full equations in the case of viscosity-dominated flows. Li *et al.* analyzed the instability of a leaky dielectric coaxial jet in both axial and radial electric fields [56,57]. The mode transitions and the effects of controllable parameters such as the inner and outer flow

rates, viscosities, surface tensions, electric intensity field and others could be predicted according to the instability analysis.

Experimental setup

Figure 1 shows a typical experimental setup for coaxial electrospray. The key component is a coaxial nozzle that consists of an outer needle and an inner needle. Two immiscible liquids, or liquid and gas, are injected into the outer and the inner needles, with the flow rates controlled by two syringe pumps, respectively. A ring-shaped electrode or a ground electrode is placed below the nozzle at a specific distance. A high voltage ranging from several kilovolts to tens of kilovolts is applied between the nozzle and the electrode. Under the elevated electric field, a Taylor cone is formed at the tip of the nozzle [27] and the jet flow of the inner and the outer liquids is eventually broken into multilayer droplets. The droplets are collected by either a ground electrode or a container underneath the electrode. A light source and camera system are used for continuous monitoring of the process.

Many existing coaxial electrospray systems are designed similar to that of Figure 1 except for minor modifications in nozzle size, needle position and electrode design. For example, Chang *et al.* used a nozzle with an inner needle of 150 μm (inner diameter [ID])/300 μm (outer diameter [OD]) and an outer needle of 685 μm (ID)/1100 μm (OD) [41]. Xie *et al.* used a bigger nozzle with an inner needle of 394 μm (ID)/720 μm (OD) and an outer needle of 2000 μm (ID)/3000 μm (OD) [23]. Tang and Gomez. found that the needle size determined the required flow rate to form a stable cone–jet mode, but had little effect on the resultant particle size [58]. A more comprehensive discussion about the influence of the needle dimension can be found in [59]. As to the needle position, some researchers placed the inner needle tip at the same height as the outer, while others raised the inner needle tip slightly above [38,41] or below [60] the outer one. In terms of the electrode design, some researchers placed a ring-shaped electrode underneath the nozzle with a distance of several millimeters to tens of millimeters, while others placed a ground electrode of a large surface area underneath the nozzle with a distance of several centimeters. Table 1 lists several experimental configurations for coaxial electrospray.

Another important aspect of experimental design in coaxial electrospray is particle collection. Unlike an emulsification process where the particles are collected by successive steps of presolidification (e.g., stirring), purification (e.g., centrifugation) and solidification (e.g., lyophilization), coaxial electrospray does not have a mature method for particle collection yet. Some researchers sprayed the particles directly on an aluminum foil that was also served as a ground electrode [23,61]. Others sprayed the particles into a glass vial placed above or under the ground electrode [17,38,41]. Since these methods combine solvent evaporation, shell hardening and particle collection within a one-step procedure, they have several limitations. First, the morphology of the produced particles cannot be effectively controlled owing to the lack of purification and the incomplete hardening of the droplets before collection. Second, the electrical, hydrodynamic and impact forces applied on the fast moving droplets may cause the significant deformation of the produced particles. Finally, the one-step procedure for particle collection cannot be scaled for mass production owing to possible particle binding and aggregation. Other particle collection methods have been explored to overcome these limitations. For example, Wang *et al.* used a rotating barrel to collect coaxial electrosprayed particles continuously [62]. Mei *et al.* introduced an air flow to suppress the possible corona discharge and a neutralization chamber to reduce the particle charges [53]. Bocanegra *et al.* developed a cooling pipe and a vacuum pump to help collection [63]. Readers who are interested in particle collection may also refer to [64–66]. Although the methods described in these references are based on single-axial electrospray,

they may provide some useful guidance for the design of the particle collection system in coaxial electrospray.

Process parameters

Coaxial electrospray is a multiphysical procedure whose outcome is affected by multiple design, process and material parameters. The applied voltage and the flow rates are the two most commonly studied process parameters contributing to droplet size, cone–jet stability, shell thickness and other performance characteristics of the process.

Applied voltage

The voltage applied between the nozzle and the electrode in a coaxial electrospray process plays an important role in the formation of a stable cone–jet. Chen *et al.* observed the transition of the following five modes as the applied voltage increased gradually: dripping mode, dripping mode in spindle, cone–jet mode, pulse mode in cone and multijet mode [67]. Mei *et al.* defined the jet-flow transition as the following four modes: dripping mode, silver-bullet mode, compound cone–jet mode and unstable cone–jet mode [54]. We observed the transition of the following four modes as the applied voltage increased: dripping mode, coning mode, stable cone–jet mode and multiet mode (Figure 2). At a stable cone–jet mode, the Taylor cone formed by both of the inner liquid and the outer liquid typically shows a symmetric shape with a thin jet at its apex. The thin jet is then broken into fine particles under the electrical and hydrodynamic forces. Chang *et al.* studied the correlation of the process parameters and the droplet characteristics in coaxial electrospray [68]. Depending on the properties and the flow rates of the inner and the outer fluids, the stable cone–jet mode is only available at a certain range of the applied voltages (Figure 3A). Within this range, the size of the formed droplets reduces as the applied voltage increases (Figure 3B).

Flow rate

In addition to the applied voltage, the inner and the outer flow rates in coaxial electrospray also play an important role in cone–jet stability and droplet size, as shown in Figure 3C. Mei *et al.* found that a stable core-shell structure could be formed for the selected inner/outer liquid combinations at the specific flow conditions [53]. Chen *et al.* found that, for the outer driving liquid, the working range of the applied voltages could be broadened by increasing the inner flow rate and by decreasing the outer flow rate [67]. It was also observed that the droplet size decreased as the flow rate decreased, which could be explained by less electric force required to overtake the hydrodynamic forces at a low flow rate [38].

Material properties

Material selection for the inner and the outer liquids in coaxial electrospray will significantly affect the cone–jet stability. Table 2 lists the reported inner/outer liquid combinations and the process information for successful coaxial electrospray. Readers may also refer to [69] for a review of commonly used materials suitable for electrospray.

The most important material parameters contributing to the outcome of a coaxial electrospray process include dielectric constant, electrical conductivity, surface/interfacial tension and viscosity. Readers may also find the published data of these material properties in the reference [70]. The contributions of these material properties to the process outcome are further discussed below.

Dielectric constant & electrical conductivity

Dielectric constant (or permittivity) ε represents the material's ability to concentrate electric flux. It is measured by the ratio of the capacitance of a capacitor filled with the given material to the capacitance of an identical capacitor in a vacuum. The dielectric constant of water is around 80 at 20°C; while that of oil is typically less than 40. Electrical conductivity K represents the material's ability to accommodate the transport of electric charge. It is measured by the ratio of the magnitude of the current density to the magnitude of the electric field. The electrical relaxation time t_e is defined as a function of dielectric constant and electrical conductivity: $t_e = \varepsilon\varepsilon_0/K$, where ε_0 is the dielectric constant of vacuum.

In a coaxial electrospray system, both the inner and the outer liquids are exposed to an elevated electric field. Their electrical properties determine the applied electrohydrodynamic forces. Usually, liquid with the smaller electrical relaxation time is considered as the dominant fluid that drives the bulk fluid to form a stable cone–jet. This dominant liquid is also called the 'driving liquid' [51]. The driving liquid transfers the electrical stress to the other liquid through viscosity. In the case of the outer driving flow, the electric charge mostly accumulates outside the outer liquid; in the case of the inner driving flow, the charge is on the interface between the inner and the outer liquids. Mei *et al.* predicted that a stable cone–jet mode was easier to form in the case of inner driving where the dielectric constant of the outer liquid is less than that of the inner liquid [54]. For coaxial electrospray of water and oil, water is typically the driving liquid since its electrical conductivity is much higher than oil. Therefore, encapsulating water in oil is easier than encapsulating oil in water.

The electrical conductivity of the inner liquid can be adjusted to achieve a stable cone jet. For example, adding potassium chloride to PLGA acetonitrile solution increased the electrical conductivity from 13.2 to 61.5 μS/cm [17]. Adding dimethyl formamide to TiO_2 ethanol solution also increased the electrical conductivity significantly [71]. The concept of a driving liquid is only important in the case of two immiscible liquids. It is much easier to achieve a stable cone–jet mode using miscible or partially miscible liquids. One example is to use acetonitrile as a solvent for both the outer and the inner liquids for the fabrication of budesonide encapsulated PLGA particles [17].

Surface tension & interfacial tension

Since coaxial electrospray involves cohesive interactions between multiple phases, maintaining an appropriate equilibrium of these phases becomes a key factor for successful production of a core-shell structure. Torza and Mason established the engulfing condition of two immiscible materials in shear and electric fields [72]. According to their analysis, the following three situations (as shown in Figure 4) may occur if phase 1 (core material) and phase 3 (shell material) are brought into contact in phase 2 (air for spraying and liquid for collection): complete engulfing, partially engulfing and nonengulfing [54].

For further analysis of the above engulfing conditions, the following spreading coefficients are defined:

$$S_i = \gamma_{ji} - \left(\gamma_{ij} + \gamma_{ik}\right)$$

where γ_{ij} is the interfacial tension between phase i and j.

The engulfing conditions can be expressed as the following functions of the spreading coefficients:

- Complete engulfing: $S_1 = \gamma_{21}-(\gamma_{12}+\gamma_{13})<0$; $S_2= \gamma_{32}-(\gamma_{23}+\gamma_{21})<0$; $S_3= \gamma_{13}-(\gamma_{31}+\gamma_{32})>0$;
- Partially engulfing: $S_1<0$; $S_2<0$; $S_3<0$;
- Nonengulfing: $S_1<0$; $S_2>0$; $S_3<0$.

To ensure the successful formation of a core-shell structure, the inner and the outer liquids have to satisfy the complete engulfing condition. Mei *et al.* listed a matrix of material pairs that could form a stable cone–jet mode [54]. The interfacial tension between materials could be adjusted by adding surfactants. For example, Tween 80 was added to glycerol to change the interfacial tension, reduce particle size and polydispersivity index, and increase the stability of the operating zone for 'microbubbling' (i.e., stable cone–jet mode [22,42]). In addition to Tween 80, other commonly used surfactants for interfacial tension adjustment include polyvinyl alcohol (PVA), sodium cholate and lecithin.

Viscosity

Viscosity is a measure of the resistance of a fluid subject to deformation by either shear or tensile stress. In a coaxial electrospray process, the driving liquid transfers the electrical stress through viscosity and drives the bulk fluid to form a stable cone–jet mode [51,67]. The electrical stress is tangential to the liquid interface and points toward the vertex of the conical interface.

In an inner driving coaxial electrospray process, the electrical charge distributes at the interface of the inner and the outer liquids. Therefore, viscosity does not play a significant role in the process outcome. However, in the case of the outer driving coaxial flow, the electric charge distributes on the outer surface of the jet and the electric force mainly applies to the outer liquid. In order to form a concentric double-layer jet, the viscosity of the outer liquid should be in an appropriate range in order to efficiently transmit the electrical stress to the inner liquid and throughout the liquid bulk by viscous diffusion. If the outer liquid is not viscous enough, recirculations in the electrified meniscus will prevent the formation of a stable cone–jet mode [73]. If the outer liquid viscosity is too large, a significantly large electric field is required to overcome the viscosity and drag the liquid out for a stable cone–jet. Chen *et al.* defined an 'accelerating point' at the top part of the Taylor cone where the inner liquid started to accelerate by the dragging force [67]. The distance from the acceleration point to the vertex of the Taylor cone is defined as the 'acceleration distance'. The longer the acceleration distance is, the more stable the cone–jet becomes.

Viscosity can be adjusted by adding miscible chemicals to the solvent. For example, Tween 80 can be added to glycerol to reduce viscosity and hence extend the operating zone for stable microbubbling [22,42]. Poly(vinylpyrrolidone) can also be used to adjust the viscosity and create MPs with a porous structure [71].

Liquid concentration

Liquid concentration affects the process outcome in a multifaceted way. First of all, the solute contents of the inner and the outer liquids contribute to their viscosity, electrical conductivity and interfacial tension. Xu *et al.* showed that, by changing the concentration of PLA in dichloroethane from 1 to 5%, viscosity changes from 2.19 to 15.8 mPas (i.e., a change of 700%) [44]. Farook and Chang *et al.* showed that, by increasing PMSQ concentration in ethanol from 18 to 63%, viscosity increases from 1.8 to 53 mPas (due to increased polymer chain entanglement), but electrical conductivity decreases from 9×10^{-5} to 1×10^{-5} S/m (due to the insulating nature of PMSQ) (Figure 3D) [39,41]. Generally speaking, changing the solute concentration in an organic solution may significantly affect its viscosity but not its electrical conductivity. However, for water or inorganic solution, the

concentration of water-soluble material (especially salt) may greatly affect its electrical conductivity but not its viscosity. In most of the cases, change of the liquid concentration has a trivial effect on its surface tension.

Second, liquid concentration indirectly affects the operating zone of a stable cone–jet mode. In particular, maintaining the outer liquid concentration within a designated range will facilitate the hard shell formation in coaxial electrospray. If the polymer concentration is too low, it is hard to form an intact shell. If the polymer concentration is too high, it is hard to achieve a stable cone–jet mode. A detailed discussion on the concentration range for PLA–BSA particle fabrication can be found in [44].

Finally, liquid concentration affects the size, the shell thickness and the core–shell thickness ratio of the fabricated particles. This effect can be exemplified by coaxial electrospray of MPs with a PMSQ shell and a perfluorohexane core [41]. By changing the PMSQ concentration (in ethanol) from 18 to 36%, the particle size increased from 460 to 630 nm, the shell thickness increased from 45 to 95 nm, and the size over thickness ratio decreased from 10.2 to 6.6.

Analytical & numerical models

Coaxial electrospray is an important branch of electrohydrodynamics that concerns the fluid dynamics with the electric force effects. To create and maintain a steady cone–jet mode in coaxial electrospray is a complex process that requires appropriate equilibrium of different forces. Since coaxial electrospray has many potential advantages over other microencapsulation/nanoencapsulation processes, it is of great interest to study the multiphysical mechanism and derive the analytical and numerical models for this process.

Formulation

To better understand the governing mechanism of coaxial electrospray, it is important to establish a theoretical framework in advance. The complete set of governing equations can be given by the fluid dynamic equations (i.e., the Navier-Stokes equations) and the electrical equations (i.e., the Maxwell's equations). For Newtonian fluids of uniform constitution, the governing equations for each phase can be expressed as:

$$\frac{1}{\rho}\frac{\mathrm{d}\rho}{\mathrm{dt}}+\nabla\vec{\mathrm{u}}=0 \quad (1)$$

$$\rho\frac{\mathrm{d}\vec{\mathrm{u}}}{\mathrm{dt}}=-\nabla\mathrm{p}+\mu\nabla^2\vec{\mathrm{u}}+\rho\vec{\mathrm{g}}+\vec{\mathrm{f}}_e \quad (2)$$

$$\nabla\vec{\mathrm{D}}=\mathrm{q},\ \nabla\vec{\mathrm{B}}=0,\ \nabla\times\vec{\mathrm{E}}=-\frac{\partial\vec{\mathrm{B}}}{\partial\mathrm{t}},\ \nabla\times\vec{\mathrm{H}}=\vec{\mathrm{J}}+\frac{\partial\vec{\mathrm{D}}}{\partial\mathrm{t}} \quad (3)$$

where the notation $\mathrm{d}/\mathrm{dt} = \partial/\partial t + \vec{\mathrm{u}}\nabla$ is the material derivative and the quantities ρ, $\vec{\mathrm{u}}$, p, μ, $\vec{\mathrm{g}}$, $\mathrm{f_e}$, D, q, B, E, H and J stand for the density, velocity vector, pressure, dynamic viscosity, gravitational acceleration, electric force, electric displacement vector, free charge density, magnetic induction, electric intensity field, magnetic intensity field and conduction current density, respectively. Equation 1 represents the conservation of mass; Equation 2 expresses the momentum equation and Equation 3 show the well-known Maxwell's equations.

The above equations can be simplified with reasonable assumptions. In most studies, the liquids and the gas can be considered as incompressible fluids. Thus Equation 1 is simplified as $\nabla\vec{u}=0$. For simplicity, the linearly constitutive relations $D=\mu E$, $B=\zeta H$ and $J=KE$ are introduced, with μ, ζ and K standing for permittivity, permeability and electrical conductivity, respectively. Since the magnetic field is very weak, the Maxwell's equations can be simplified as the following: $\nabla D=q$, $\nabla \times E = 0$, $\partial p/\partial t + \nabla J=0$. The detailed derivation of the governing equations can be found in [74,75].

In electrohydrodynamics problems, the electric force affects the movement of fluids, which changes the distribution of charges within the fluids and on the interfaces. Therefore, the electric force is coupled with surface/interface tension, viscous force, inertia force and so on. Considering that there are two interfaces in a coaxial electrospray problem, the kinematic, dynamic and electrical boundary conditions are required for each interface.

The kinematic interface condition for each interface can be written as:

$$\frac{\partial F}{\partial t}+\vec{u}\nabla F=0 \quad (4)$$

where F is the interface function.

The dynamic boundary condition for each interface can be expressed as:

$$\left\|\vec{T}^{m}+\vec{T}^{e}\right\|\vec{n}=\gamma\nabla\vec{n}+(\delta-\vec{n}\vec{n})\nabla\gamma \quad (5)$$

where || and || indicated the jump of corresponding quantity across the interface. $\vec{T}^{m}$, $\vec{T}^{e}$, $\vec{n}$, γ and δ represent the hydrodynamic stress tensor, electrical Maxwell tensor, normal unit vector, surface tension and identity matrix, respectively.

The electrical boundary conditions for each interface can be given by:

$$\vec{n}\left\|\vec{D}\right\|=q_s \quad (6)$$

$$\vec{n}\times\left\|\vec{E}\right\|=0 \quad (7)$$

Equation 6 expresses the Gauss law in which the surface charge density q_s satisfies the surface charge conservation law. Equation (7) represents the continuity of the tangential component of the electric field.

For viscous fluids, the tangential component of the velocity should be continuous on the interface:

$$\vec{n}\times\left\|\vec{u}\right\|=0 \quad (8)$$

In addition to the above boundary conditions, there are other solution-dependent boundary conditions such as the finiteness of velocity and electric intensity field at the symmetric axis. These governing equations and boundary conditions are applicable in most cases no matter whether the fluids are liquids or gases.

It must be pointed out that solving the above problem is very difficult because of the following challenges: the two interfaces of the problem are unknown, the length scales of the capillary needles and the jets are very disparate, and the breakup of jets is time dependent. Therefore, modeling a coaxial electrospray process is a complicated procedure involving a larger number of unknowns and parameters. Further simplifications and assumptions are necessary in order to study the coaxial electrified jet under either the outer-driving or the inner-driving flow conditions. This is different from a single-axial electrospray process where analytical and numerical models can be obtained and the key process parameters can be analyzed systemically.

Scaling law

Since the cone and the jet are in disparate scales, they are usually studied separately. As for the cone, Marin *et al.* studied the coaxial electrospray within a bath containing a dielectric liquid and observed that a sharp tip in the inner dielectric meniscus would be formed without mass emission [52]. They presented an analytical model of the flow in the inner and the outer menisci based on different simplifying hypotheses. The fluid dynamic equations were simplified in a low Reynolds number limit and under the assumption that the electrical effects inside the liquid bulk were negligible. The electrical equations were also reduced into the Laplace equation of the electric field. After the boundary conditions on the two interfaces were applied and the assumptions of self-similarity and very thin conductive layer were made, the velocity, the pressure fields and the electrical shear stress at the outer surface were finally calculated. As for the jet and the resulting droplets, Lopez-Herrera *et al.* derived the scaling laws of the diameter of the coaxial electrified jet and the current transported throughout the jet by experimenting with different liquids, such as water, sunflower oil, ethylene-glycol and Somos [51]. The dimensionless parameters were defined based on the reference characteristic values of the flow rate Q_0, the current I_0, and the diameter d_0, as given by:

$$Q_0=\frac{\gamma_{\text{eff}}\varepsilon_0}{\rho\sigma}, I_0=\left(\frac{\gamma^2_{\text{eff}}\varepsilon_0}{\rho}\right)^2, d_0=\left(\frac{Q_0\varepsilon_0}{\sigma}\right)^{1/3} \quad (9)$$

where γ_{eff} denotes the effective value of the surface tension. The results indicated that the current I/I_0 on the driving flow rate Q/Q_0 closely followed a power law of $(Q/Q_0)^{1/2}$, similar to that in single-axial electrospray. It was also found that the mean diameter of the droplets resulted from the breakup of the coaxial jets scaled linearly with both inner and outer flow rates in the case of outer driving; whereas that diameter was closely dependent of the ratio of inner and outer flow rates in the case of inner driving. Marín *et al.* obtained the diameter of the coaxial jets d as a function of the flow rate Q [52]. They found that the experimental results fitted in the $Q^{1/2}$ law as below:

$$\frac{d}{d_0}=1.25(Q/Q_0)^{1/2} \quad (10)$$

Mei *et al.* found the particle encapsulation conditions relevant with the flow rates and the material properties in the case of the inner driving flow [53]. Let r* be the charge relaxation length and R* be the inertial length:

$$r^*=(Q\varepsilon\varepsilon_0/\sigma)^{1/3}, R^*=(\rho Q^2/\gamma)^{1/3} \quad (11)$$

The particle encapsulation conditions were therefore expressed as:

$$r_O^*/r_I^*<500, R_O^*/R_I^*<0.015 \quad (12)$$

where the subscripts O and I indicate the outer liquid and the inner liquid, respectively.

Furthermore, the flow rates of the inner needle and outer needle may affect the range of the stable cone–jet, and thus affect the jet size and the particle size. Chen *et al.* found that the working range for the stable cone–jet could be expanded by increasing the inner liquid flow rate and by decreasing the outer liquid flow rate in the case of outer driving [67]. It has been shown previously that the particle size decreases as the applied voltage increases in a stable cone–jet mode. Similar reduction of the particle size can also be achieved by reducing the flow rate, which can be explained by easier overtaking of the electrical force over the hydrodynamic forces in reduction of flowing materials [21]. In practice, stable cone–jet mode should be adjusted at the higher applied voltage and lower flow rates in order to get the smaller particle size.

Instability analysis

It is well known that the breakup of liquid jets is closely associated with the jet instability [76–78]. Therefore, the hydrodynamic instability theory can be used for coaxial electrospray analysis and has successfully predicted the experimental observations [56,57]. The instability theory deals with the mathematical analysis of the response of disturbances with small amplitudes superposed on a laminar basic flow. If the flow returns to its original laminar state, it is recognized as stable. However, if the disturbance grows and the flow changes into a different state, it is recognized as unstable. When analyzing the instability problems, the governing equations and the boundary conditions described above are used and the classical method of expansion of normal modes is usually implemented. This method analyzes the development of perturbations in space only, in time only, or in both space and time. The analysis results may provide theoretical insight and practical guidance for coaxial electrospray process control.

For instability analysis in a cylindrical coordinate (z, r, θ), the arbitrary and independent perturbations are typically decomposed into Fourier series like $\exp\{\omega t+i(kz+n\theta)\}$, where ω, k and n stand for the frequency, the axial wave number and the azimuthal wave number, respectively. In the case of coaxial electrospray, a local temporal method is used for instability analysis. This method assumes a real axial wave number and pursues a complex frequency since its linear dispersion relation is relatively easy to solve. To the best of the authors' knowledge, this is the most commonly used method so far for instability analysis of coaxial electrospray. Other methods are waiting for development in the future. Li *et al.* studied the instability of an inviscid coaxial jet under an axial electric field [57]. They also studied the axisymmetric and nonaxisymmetric instabilities of a viscous coaxial jet under a radial electric field [56]. These studies solved the governing equations and boundary conditions based on a number of assumptions and simplifications, such as: the inner and the outer liquids were assumed to be perfect conductors, perfect dielectrics or leaky dielectrics; the free charges were relaxed to the interface instantaneously, and the effects of gravitational acceleration and temperature were ignored. Figure 5 sketches a simplified physical model for coaxial electrospray. It consists of a cylindrical inner liquid 1 of radius R_1, an annular outer liquid 2 of outer radius R_2, and an ambient gas 3 that is stationary air in an unperturbed state. The basic flows should be assumed uniform or with specific shapes. Si *et al.* used the uniform velocities U_i with i = 1, 2, 3 for the inner liquid, the outer liquid and the ambient gas (in this case $U_3 = 0$) and the uniform axial electric field E_0 [79]. The corresponding dispersion relations were derived and written in an explicit analytical form, and the eigenvalues were computed by numerical methods. In general, the dispersion relation could be expressed in the form of:

$$f(\omega, k, n, U_i, E_0, \varepsilon, K, \ldots)=0 \quad (13)$$

An example of instability results is presented in Figure 6. The involved dimensionless parameters include: dimensionless wave number $\alpha = kR_2$, dimensionless frequency $\beta = \omega R_2/U_2$, Weber number $We = \rho_2 U_2^2 R_2/\gamma_2$, dimensionless electrostatic force $E = \varepsilon_3 E_0^2/\rho_2 U_2^2$, density ratios $S = \rho_1/\rho_2$ and $Q = \rho_3/\rho_2$, velocity ratio $U = U_1/U_2$, diameter ratio $R = R_1/R_2$, electric permittivity ratios $\varepsilon_{1P} = \varepsilon_1/\varepsilon_3$ and $\varepsilon_{2P} = \varepsilon_2/\varepsilon_3$, conductivity ratio $K = K_1/K_2$, and interfacial tension coefficient ratio $\gamma = \gamma_1/\gamma_2$ [79]. The instability analysis yielded the following three unstable modes: paravaricose mode, parasinuous mode and transitional mode. The paravaricose mode occurs when the phase difference of initial perturbations at the inner and the outer interfaces was about 180°. The parasinuous mode occurs at a phase difference of approximately 0°. The transitional mode occurs when the initial perturbation is changed from in phase to out of phase. In particular, the maximal growth rate of dimensionless frequency β_{rmax} dominates the jet breakup because the perturbation for β_{rmax} grows most quickly (i.e., the perturbation grows exponentially in the dimensional form of $\exp\{\omega_r t\}$). The corresponding axial wave number α_{max} plays an important role in fabricating MPs and NPs because the wave number is closely associated with the wavelength of perturbations (i.e., $\alpha = 2\pi R_2/\lambda$, where λ stands for the wavelength). The larger α_{max} is, the smaller the size of resulting MPs and NPs becomes. As a result, Equation 13 allows us to study the effects of the electric field, the electrical conductivity, the electrical permittivity and the other important hydrodynamic parameters on the instability of the coaxial jet. It also allows us to predict the different flow modes and the corresponding transitions.

MPs & NPs fabricated by coaxial electrospray

Methods for particle characterization

In order to evaluate the outcome of a coaxial electrospray process and facilitate its potential applications in producing drug-loaded MPs and NPs, it is necessary to characterize the physical and chemical properties of the fabricated particles quantitatively. This section describes the commonly used tools and methods to verify the core-shell structure, to characterize the morphology, to estimate the size distribution, and to evaluate the chemical compositions of the coaxial electrosprayed MPs and NPs.

Verification of core-shell structure—Confocal fluorescence microscopy is one of the most commonly used imaging modalities to verify the core-shell structure of multilayered MPs [17,62,80]. Wang *et al.* stained the BSA core with fluorescein isothiocyanate and stained the PLGA shell with rhodamine-B for confocal fluorescence microscopic imaging of IGF-1 loaded microspheres [62], as shown in Figure 7. Other commonly used dyes include rhodamine B [37,62] and coumarin-6 [37,80] for the organic solvents, fluorescein sodium salt [17], fluorescein isothiocyanate [62] and rhodamine B [80] for the inorganic solvents, and Nile red for both organic and inorganic solvents [63].

In addition to confocal fluorescence microscopy, other methods have also been used to confirm the particle core-shell structure. For example, transmission electron microscopy was used to detect the core-shell structure of budesonide/EGCG-loaded PLGA MPs [17,81]. Energy-dispersive x-ray spectroscopy was used to indirectly confirm the core-shell structure and characterize the presence of Zr and Al elements in the core and shell of zirconia/alumina MPs [82,83].

Characterization of particle morphology—Scanning electron microscopy (SEM) has been commonly used to characterize the morphologic features of coaxial electrosprayed particles [17,39,80,84]. Figure 8 shows the SEM images of the Budesonide-loaded PLGA MPs and NPs at different concentrations [17]. Figure 9 shows the SEM images of these particles at different release stages [17].

Measurement of size distribution & zeta potential—The size distribution of MPs and NPs can be characterized by many methods such as microscopy, flow cytometry and dynamic light scattering (DLS) [85]. DLS is also known as photon correlation spectroscopy or quasielastic light scattering. It detects the hydrodynamic diameter of small particles in suspension by measuring the intensity fluctuation of the scattered light due to Brownian motion. Zeta potential is the electrokinetic potential (i.e., the surface charge) of the particles that can be detected by either the microelectrophoresis or the electrophoretic light scattering method. It indicates the degree of repulsion between adjacent, similarly charged particles in dispersion. Size distribution and zeta potential are important characteristics because they directly affect the delivery and binding efficiencies of many MPs and NPs for *in vivo* drug delivery applications.

Characterization of chemical composition—Commonly used methods to characterize the chemical composition of drug-loaded MPs and NPs include Raman spectroscopy [50], Fourier transform infrared spectroscopy [44,84] and differential mobility spectroscopy [21]. In addition, the differential scanning calorimetry method was used to characterize PLA/BSA MPs by checking the thermal behavior of PLA and the physical status of BSA [44]. Circular dichroism spectroscopy was used to determine the secondary structure of BSA and evaluate the protein difference before electrospray and after release [23]. Gel electrophoresis was used to characterize the encapsulation efficiency of an oligode-oxynucleotide G3139 in lipoplex particle [61]. UV spectroscopy [84] and HPLC [17,45] were also used to characterize the *in vitro* release profiles of the coxial electrosprayed MPs and NPs.

Coaxial electrosprayed MPs & NPs

Since the first report of coaxial electrospray in 2002, many research efforts have been made for the further advancement of this microencapsulation/nanoencapsulation technique. Table 2 summarizes the MPs and NPs fabricated by coaxial electrospray. In addition to the two-layer MPs and NPs, particles with multiple layers and complicated structures have also been produced. Ahmad *et al.* fabricated MPs with three concentric layers using a novel trineedle coaxial device [49]. The size of these MPs is in the range of 50–200 μm, with a structure of either air/glycerol/olive oil or BSA/starch/polyurethane (from inside to outside). Lee *et al.* and Kim *et al.* also reported the three-layer MPs with the size of several micrometers [17,50]. Chen *et al.* fabricated MPs of around 10 μm that contain three or four inner compartments by positioning three or four capillaries inside an outer needle [81,86]. These multicompartment MPs may be potentially used for controlled release of multiple drug components.

In comparison with a double-emulsion technique, coaxial electrospray has the potential to encapsulate drugs and reagents with high efficiency. For example, an encapsulating efficiency of 65–75% was achieved for coaxial electrospray of oestradiol-loaded PLGA capsules [24]. Lee *et al.* even reported an encapsulation efficiency of greater than 90% for budesonide-loaded PLGA MPs [17]. Wu *et al.* also reported a similarly high encapsulation efficiency for loading oligodeoxynucleotide G3139 in lipoplex [61].

A double-emulsion process may demolish the bioactivity of the encapsulated payloads. In comparison, a coaxial electrospray process has the potential to preserve the payload

bioactivity, making it especially useful for encapsulating genes, antibodies and other protein drugs. In an *in vitro* experiment conducted by Xie *et al.*, the bioactivity of lysozyme encapsulated in PLGA MPs was greater than 90% and the encapsulated BSA was sustain-released for more than 30 days [23]. Park *et al.* also reported the preservation of lysozyme bioactivity by coaxial electrosprayed particles [80]. Wu *et al.* reported the uptake of oligodeoxynucleotide G3139 by K562 cells from lipoplex NPs [61]. Nie *et al.* fabricated paclitaxel and suramin-loaded MPs to treat subcutaneous U87 glioma xenograft in BALB/c nude mice [45]. Wu *et al.* used coaxial electrospray to produce nonviral vectors of DNA/PEI polyplexes and demonstrated more control over the traditional fabrication method (bulk mixing) [85]. Jayasinghe *et al.* encapsulated immortalized human astrocytoma cell line 1321N1 in 30 μm microdroplets and the cells stayed alive during the electrospray process [87]. Other coaxial electrosprayed MPs and NPs for *in vitro* and *in vivo* release tests can be found in references [17,23,24,71,80].

In addition to drug delivery applications, coaxial electrospray has also been used for encapsulating a variety of reagents for many different applications. For example, Jing *et al.* fabricated multifunctional MPs with a TiO_2 shell and a core of Fe_3O_4, paclitaxel and grapheme quantum dots for MRI, fluorescence imaging, ultrasonography and triggered drug delivery [71]. Bocanegra *et al.* encapsulated water in cocoa butter by coaxial electrospray in order to demonstrate the targeted melting and release of cocoa butter at body temperature without being broken upon mastication [63].

Expert commentary

Coaxial electrospray is a novel microencapsulation/nanoen-capsulation technique with a short history. It produces multilayer MPs and NPs with a core-shell structure by introducing electrified coaxial jets. This process has several advantages over other commonly used microencapsulation/nanoencapsulation processes. First of all, coaxial electrospray is a versatile process with a broad selection of core-shell materials and a nearly 100% encapsulation rate. It is especially useful for encapsulating water-soluble reagents since the process can effectively protect water-soluble payloads from diffusion or other process-induced loss. In comparison, commonly used encapsulation processes such as double emulsion have low efficiency for encapsulating water-soluble payloads. With coaxial electrospray, it is even possible to encapsulate solid drug suspensions or drug-loaded NPs for long-term sustained release. Second, this process protects biologically active payloads from process-induced damage. Unlike an emulsification process where the process-induced mechanical forces and reagents may cause protein denaturation or bioactivity reduction, coaxial electrospray introduces an elevated electrical field with minimal biological side effects. Therefore, the process is ideal for encapsulating cells and various biological agents, such as genes and antibodies. Finally, this process has the potential to control particle morphology with flexibility and reproducibility. On the one hand, particles with uniform size distributions can be fabricated at both microscales and nanoscales. On the other hand, multiple imaging and therapeutic agents can be encapsulated in different compartments of a biodegradable carrier for multimodal imaging and synergistic therapy. In summary, coaxial electrospray opens a new avenue for microencapsulation/nanoencapsulation of imaging and therapeutic agents, with the potential of improving their encapsulation and delivery efficiencies significantly.

Although coaxial electrospray is a promising process with great potential, the technology is still at its early stage and requires further research and development. On the experimental side, many reported works in coaxial electrospray are based on individual laboratory experience, specific material combinations and empirical process parameters. Reliable and reproducible fabrication of multilayer MPs and NPs is hindered by the lack of standard

protocols and the lack of a systemic process control. Mass production of multilayer MPs and NPs is hindered by the lack of an effective particle collection method and the lack of a more productive nozzle design. In terms of particle collection, commonly used one-step collection methods cannot facilitate shell hardening, or maintain particle morphology or prevent particle aggregation. Therefore, more effective particle collection methods have to be developed. In terms of nozzle design, the existing single-nozzle system limits the productivity significantly and a micro machined coaxial nozzle array is necessary. On the modeling and theoretical side, many existing process models are either empirical or semiquantitative. The simulated results are not sufficient for quantitative process control. Numerical simulations such as computational fluid dynamics modeling has been used to simulate the liquid cone formation and atomization in a single axial electrospray process [88]. However, the computational fluid dynamics model cannot be directly implemented in coaxial electrospray owing to the multiphysical nature of the process and the complicated interfacial interactions of the multilayer jets. Instability analysis is a promising tool to predict process outcome without introducing computational complexity. However, the instability model makes a number of simplifications and assumptions to the real process. Consequently, the theoretical results obtained from the instability analysis may be qualitatively consistent with those of experiments, but may not match the experimental observations quantitatively. Further experimental, theoretical and numerical studies are needed in the future in order to better understand the physical nature of coaxial electrospray and provide quantitative guidance for process control.

Five-year view

Coaxial electrospray is an emerging technique with only 10 years of history. Although the technique has multiple advantages over traditional microencapsulation/nanoencapsulation processes, further advancement is challenged by the complex physics of the process and a large number of design, material and process parameters contributing to the process outcome. Current research efforts on coaxial electrospray focus on concept approval and feasible study, with about 100 journal papers published by major research groups. The published results are typically based on individually customized experimental setups, a limited number of material combinations and empirical process parameters. Some of the published studies have not been systemically designed and the results are sometimes incomparable. The researchers working in this area can be categorized into two groups. The first group is biomedical engineers and clinical researchers who are interested in encapsulating biological agents for specific imaging and therapeutic applications. The second group includes experimentalists and theorists in the field of fluid mechanics who are interested in experimental and modeling works associated with coaxial electrospray. In the next 5 years, we expect to see seamless collaborations between these two groups of researchers to accelerate technology development and dissemination from research laboratories to clinical applications. We also expect systemic and standardized studies carried out on both the experimental and the theoretical sides of coaxial electrospray by more and more multidisciplinary research groups. We further expect the partnership among research laboratories, biomedical industry and government agencies for standardization and technology commercialization of this novel microencapsulation/nanoencapsulation process with great potential.

Acknowledgments

Fruitful discussions with Fang Li and insightful guidance from Cynthia Roberts are greatly appreciated.

References

Papers of special note have been highlighted as:

• of interest

1. Mundargi RC, Babu VR, Rangaswamy V, Patel P, Aminabhavi TM. Nano/micro technologies for delivering macromolecular therapeutics using poly(D,L-lactide-co-glycolide) and its derivatives. J Control Release. 2008; 125(3):193–209. [PubMed: 18083265]
2. Hall JB, Dobrovolskaia MA, Patri AK, McNeil SE. Characterization of nanoparticles for therapeutics. Nanomedicine (Lond). 2007; 2(6):789–803. [PubMed: 18095846]
3. Bourges JL, Gautier SE, Delie F, et al. Ocular drug delivery targeting the retina and retinal pigment epithelium using polylactide nanoparticles. Invest Ophthalmol Vis Sci. 2003; 44(8):3562–3569. [PubMed: 12882808]
4. de Jalón EG, Blanco-Príeto MJ, Ygartua P, Santoyo S. PLGA microparticles: possible vehicles for topical drug delivery. Int J Pharm. 2001; 226(1–2):181–184. [PubMed: 11532580]
5. Byrne JD, Betancourt T, Brannon-Peppas L. Active targeting schemes for nanoparticle systems in cancer therapeutics. Adv Drug Deliv Rev. 2008; 60(15):1615–1626. [PubMed: 18840489]
6. Veronese FM, Pasut G. PEGylation, successful approach to drug delivery. Drug Discov Today. 2005; 10(21):1451–1458. [PubMed: 16243265]
7. Betancourt T, Byrne JD, Sunaryo N, et al. PEGylation strategies for active targeting of PLA/PLGA nanoparticles. J Biomed Mater Res A. 2009; 91(1):263–276. [PubMed: 18980197]
8•. Schneider M, Bussat P, Barrau MB, Arditi M, Yan F, Hybl E. Polymeric microballoons as ultrasound contrast agents. Physical and ultrasonic properties compared with sonicated albumin. Invest Radiol. 1992; 27(2):134–139. First coaxial electrospray paper published. [PubMed: 1376304]
9. Pisani E, Tsapis N, Galaz B, et al. Perfluorooctyl bromide polymeric capsules as dual contrast agents for ultrasonography and magnetic resonance imaging. Adv Funct Mat. 2008; 18:2963–2971.
10. Kim C, Erpelding TN, Maslov K, et al. Handheld array-based photoacoustic probe for guiding needle biopsy of sentinel lymph nodes. J Biomed Opt. 2010; 15(4):046010. [PubMed: 20799812]
11. Xu RX, Huang J, Xu JS, et al. Fabrication of indocyanine green encapsulated biodegradable microbubbles for structural and functional imaging of cancer. J Biomed Opt. 2009; 14(3):034020. [PubMed: 19566313]
12. Gao Z, Kennedy AM, Christensen DA, Rapoport NY. Drug-loaded nano/microbubbles for combining ultrasonography and targeted chemotherapy. Ultrasonics. 2008; 48(4):260–270. [PubMed: 18096196]
13. Xu RX, Xu JS, Zuo T, Shen R, Huang TH, Tweedle MF. Drug-loaded biodegradable microspheres for image-guided combinatory epigenetic therapy in cells. J Biomed Opt. 2011; 16(2):020507. [PubMed: 21361663]
14. Fernandez-Fernandez A, Manchanda R, McGoron AJ. Theranostic applications of nanomaterials in cancer: drug delivery, image-guided therapy, and multifunctional platforms. Appl Biochem Biotechnol. 2011; 165(7–8):1628–1651. [PubMed: 21947761]
15. Astete CE, Sabliov CM. Synthesis and characterization of PLGA nanoparticles. J Biomater Sci Polym Ed. 2006; 17(3):247–289. [PubMed: 16689015]
16. Jain RA. The manufacturing techniques of various drug loaded biodegradable poly(lactide-co-glycolide) (PLGA) devices. Biomaterials. 2000; 21(23):2475–2490. [PubMed: 11055295]
17. Lee YH, Mei F, Bai MY, Zhao S, Chen DR. Release profile characteristics of biodegradable-polymer-coated drug particles fabricated by dual-capillary electrospray. J Control Release. 2010; 145(1):58–65. [PubMed: 20346381]
18. PHOTONIFY TECHNOLOGIES. US0035317. 2001.
19. Xu JS, Huang J, Qin R, et al. Synthesizing and binding dual-mode poly (lactic-co-glycolic acid) (PLGA) nanobubbles for cancer targeting and imaging. Biomaterials. 2010; 31(7):1716–1722. [PubMed: 20006382]

20. Putney SD, Burke PA. Improving protein therapeutics with sustained-release formulations. Nat Biotechnol. 1998; 16(2):153–157. [PubMed: 9487521]
21. Loscertales IG, Barrero A, Guerrero I, Cortijo R, Marquez M, Gañán-Calvo AM. Micro/nano encapsulation via electrified coaxial liquid jets. Science. 2002; 295(5560):1695–1698. [PubMed: 11872835]
22. Farook U, Stride E, Edirisinghe MJ. Stability of microbubbles prepared by co-axial electrohydrodynamic atomisation. Eur Biophys J. 2009; 38(5):713–718. [PubMed: 19132365]
23•. Xie J, Ng WJ, Lee LY, Wang CH. Encapsulation of protein drugs in biodegradable microparticles by co-axial electrospray. J Colloid Interface Sci. 2008; 317(2):469–476. Proved that coaxial electrospray has advantages for encapsulating sensitive proteins. [PubMed: 17945246]
24. Enayati M, Ahmad Z, Stride E, Edirisinghe M. One-step electrohydrodynamic production of drug-loaded micro- and nanoparticles. J R Soc Interface. 2010; 7(45):667–675. [PubMed: 19828501]
25. Zeleny J. The electrical discharge from liquid points, and a hydrostatic method of measuring the electric intensity at their surfaces. Phys Rev. 1914; 3(2):69–91.
26. Zeleny J. Instability of electrified liquid surfaces. Phys Rev. 1917; 10(1):1–6.
27•. Taylor G. Disintegration of water drops in an electric field. Proc R Soc A-Math Phys Eng Sci. 1964; 280(1382):383. Fundamental publication in electrospray.
28. Delamora JF. The fluid dynamics of Taylor cones. Annu Rev Fluid Mech. 2007; 39:217–243.
29. Fenn JB, Mann M, Meng CK, Wong SF, Whitehouse CM. Electrospray ionization for mass spectrometry of large biomolecules. Science. 1989; 246(4926):64–71. [PubMed: 2675315]
30. Schmitt-Kopplin P, Frommberger M. Capillary electrophoresis-mass spectrometry: 15 years of developments and applications. Electrophoresis. 2003; 24(22–23):3837–3867. [PubMed: 14661221]
31. Khaledi, MG. High Performance Capillary Electrophoresis: Theory, Techniques, and Applications. Wiley; NY, USA: 1998.
32. Fenn JB, Mann M, Meng CK, Wong SF, Whitehouse CM. Electrospray ionization – principles and practice. Mass Spect Rev. 1990; 9(1):37–70.
33. Sato M, Kuroiwa I, Ohshima A. Production of nanosilica particles in liquid–liquid system by pulsed voltage application. IEEE Trns Dielectr Electr Insul. 2009; 16(2):320–324.
34. Sato M, Okubo N, Nakane T, Sun B, Urashima K. Nozzleless EHD Spraying for fine droplet production in liquid-in-liquid system. IEEE Trans Ind Appl. 2010; 46(6):2190–2195.
35. Xie J, Wang CH. Encapsulation of proteins in biodegradable polymeric microparticles using electrospray in the Taylor cone–jet mode. Biotechnol Bioeng. 2007; 97(5):1278–1290. [PubMed: 17216662]
36. Xu Y, Hanna MA. Electrospray encapsulation of water-soluble protein with polylactide. Effects of formulations on morphology, encapsulation efficiency and release profile of particles. Int J Pharm. 2006; 320(1–2):30–36. [PubMed: 16697538]
37. Hwang YK, Jeong U, Cho EC. Production of uniform-sized polymer core-shell microcapsules by coaxial electrospraying. Langmuir. 2008; 24(6):2446–2451. [PubMed: 18257594]
38•. Farook U, Stride E, Edirisinghe MJ, Moaleji R. Microbubbling by co-axial electrohydrodynamic atomization. Med Biol Eng Comput. 2007; 45(8):781–789. A representative publication that covers bother experimental and theoretical works. [PubMed: 17624564]
39. Pancholi KP, Farook U, Moaleji R, Stride E, Edirisinghe MJ. Novel methods for preparing phospholipid coated microbubbles. Eur Biophys J. 2008; 37(4):515–520. [PubMed: 17687548]
40. Farook U, Stride E, Edirisinghe MJ. Preparation of suspensions of phospholipid-coated microbubbles by coaxial electrohydrodynamic atomization. J R Soc Interface. 2009; 6(32):271–277. [PubMed: 18647738]
41•. Chang MW, Stride E, Edirisinghe M. A new method for the preparation of monoporous hollow microspheres. Langmuir. 2010; 26(7):5115–5121. First paper in co-axial electrospray that analyzed the thickness of the shell with key parameters. [PubMed: 20095539]
42. Farook U, Stride E, Edirisinghe MJ. Controlling size and size distribution of electrohydrodynamically prepared microbubbles. Bubble Sci Eng Technol. 2009; 1(2):53–57.

43. Farook U, Zhang HB, Edirisinghe MJ, Stride E, Saffari N. Preparation of microbubble suspensions by co-axial electrohydrodynamic atomization. Med Eng Phys. 2007; 29(7):749–754. [PubMed: 17035065]
44. Xu Y, Hanna MA. Morphological and structural properties of two-phase coaxial jet electrosprayed BSA-PLA capsules. J Microencapsul. 2008; 25(7):469–477. [PubMed: 18608807]
45. Nie H, Fu Y, Wang CH. Paclitaxel and suramin-loaded core/shell microspheres in the treatment of brain tumors. Biomaterials. 2010; 31(33):8732–8740. [PubMed: 20709388]
46. Wu Y, Li L, Mao Y, Lee LJ. Static micromixer-coaxial electrospray synthesis of theranostic lipoplexes. ACS Nano. 2012; 6(3):2245–2252. [PubMed: 22320282]
47. Park S, Hwang S, Lee J. pH-responsive hydrogels from moldable composite microparticles prepared by coaxial electrospray drying. Chem Eng J. 2011; 169:348–357.
48. Zhang S, Kawakami K, Yamamoto M, et al. Coaxial electrospray formulations for improving oral absorption of a poorly water-soluble drug. Mol Pharm. 2011; 8(3):807–813. [PubMed: 21395264]
49. Ahmad Z, Zhang HB, Farook U, Edirisinghe M, Stride E, Colombo P. Generation of multilayered structures for biomedical applications using a novel tri-needle coaxial device and electrohydrodynamic flow. J R Soc Interface. 2008; 5(27):1255–1261. [PubMed: 18647737]
50. Kim W, Kim SS. Multishell encapsulation using a triple coaxial electrospray system. Anal Chem. 2010; 82(11):4644–4647. [PubMed: 20459114]
51•. Lopez-Herrera J, Barrero A, Lopez A, Loscertales I, Marquez M. Coaxial jets generated from electrified Taylor cones. Scaling laws. J Aerosol Sci. 2003; 34:535–552. First attempt to explain co-axial electrospray theoretically.
52. Marín AG, Loscertales IG, Márquez M, Barrero A. Simple and double emulsions via coaxial jet electrosprays. Phys Rev Lett. 2007; 98(1):014502. [PubMed: 17358479]
53•. Mei F, Chen DR. Investigation of compound jet electrospray: particle encapsulation. Phys Fluids. 2007; 19(103303):1–10. Provided the formulas to determine in which condition the core-shell structure could be formed.
54•. Mei F, Chen DR. Operational modes of dual-capillary electrospraying and the formation of the stable compound cone–jet mode. Aerosol Air Qual Res. 2008; 8(2):218–232. Provided the matrix table on forming a stable cone–jet mode.
55. Higuera FJ. Stationary coaxial electrified jet of a dielectric liquid surrounded by a conductive liquid. Phys Fluids. 2007; 19:012102.
56. Li F, Yin XY, Yin XZ. Axisymmetric and non-axisymmetric instability of an coflowing jet under an axial electrifiedc field viscous coaxial jet. J Fluid Mech. 2009; 632:199–225.
57. Li F, Yin XY, Yin XZ. Linear instability of a coflowing jet under an axial electric field. Phys Rev E Stat Nonlin Soft Matter Phys. 2006; 74(3 Pt 2):036304. [PubMed: 17025740]
58. Tang K, Gomez A. On the structure of an electrostatic spray of monodisperse droplets. Phys Fluids. 1994; 6(7):2317–2332.
59. Tetler LW, Cooper PA, Powell B. Influence of capillary dimensions on the performance of a coaxial capillary electrophoresis- electrospray mass spectrometry interface. J Chromatogr A. 1995; 700(1–2):21–26.
60. Park I, Kim W, Kim SS. Multi-jet mode electrospray for non-conducting fluids using two fluids and a coaxial grooved nozzle. Aerosol Sci Technol. 2011; 45:629–634.
61. Wu Y, Yu B, Jackson A, Zha W, Lee LJ, Wyslouzil BE. Coaxial electrohydrodynamic spraying: a novel one-step technique to prepare oligodeoxynucleotide encapsulated lipoplex nanoparticles. Mol Pharm. 2009; 6(5):1371–1379. [PubMed: 19499922]
62. Wang F, Li Z, Tamama K, Sen CK, Guan J. Fabrication and characterization of prosurvival growth factor releasing, anisotropic scaffolds for enhanced mesenchymal stem cell survival/growth and orientation. Biomacromolecules. 2009; 10(9):2609–2618. [PubMed: 19689108]
63. Bocanegra R, Gaonkar AG, Barrero A, Loscertales IG, Pechack D, Marquez M. Production of cocoa butter microcapsules using an electrospray process. J Food Sci. 2005; 70(8):e492–e497.
64. Ding L, Lee T, Wang CH. Fabrication of monodispersed Taxol-loaded particles using electrohydrodynamic atomization. J Control Release. 2005; 102(2):395–413. [PubMed: 15653160]

65. Xie J, Lim LK, Phua Y, Hua J, Wang CH. Electrohydrodynamic atomization for biodegradable polymeric particle production. J Colloid Interface Sci. 2006; 302(1):103–112. [PubMed: 16842810]
66. Almería B, Fahmy TM, Gomez A. A multiplexed electrospray process for single-step synthesis of stabilized polymer particles for drug delivery. J Control Release. 2011; 154(2):203–210. [PubMed: 21640147]
67. Chen X, Jia L, Yin X, Cheng J, Lu J. Spraying modes in coaxial jet electrospray with outer driving liquid. Phys Fluids. 2005; 17:032101.
68. Chang MW, Stride E, Edirisinghe M. Controlling the thickness of hollow polymeric microspheres prepared by electrohydrodynamic atomization. J R Soc Interface. 2010; 7(Suppl 4):S451–S460. [PubMed: 20519216]
69. Jaworek A, Sobczyk AT. Electrospraying route to nanotechnology: an overview. J Electrostat. 2008; 66(3–4):197–219.
70. Riddick, JA.; Bunger, WB.; Sakano, TK. Organic Solvents: Physical Properties and Methods of Purification. John Wiley and Sons; New York, NY, USA: 1986.
71. Jing Y, Zhu Y, Yang X, Shen J, Li C. Ultrasound-triggered smart drug release from multifunctional core-shell capsules one-step fabricated by coaxial electrospray method. Langmuir. 2011; 27(3):1175–1180. [PubMed: 21182239]
72. Torza S, Mason S. Three-phase interactions in shear and electrical fields. J Colloid Interface Sci. 1970; 33(1):67–83.
73. Barrero A, Ganan-Calvo AM, Davila J, Palacio A, Gomez-Gonzalez E. Low and high Reynolds number flows inside Taylor cones. Phys Rev E. 1998; 58(6):7309.
74. Batchelor, GK. An Introduction to Fluid Dynamics. Cambridge University Press; England, UK: 2000.
75. Castellanos, A. Electrohydrodynamics. Springer-Verlag; Wien, NY, USA: 1998.
76. Lin, SP. Breakup of Liquid Sheets and Jets. Cambridge University Press; England, UK: 2003.
77. Si T, Li F, Yin XY, Yin XZ. Modes in flow focusing and instability of coaxial liquid–gas jets. J Fluid Mech. 2009; 629:1–23.
78. Si T, Li F, Yin XY, Yin XZ. Spatial instability of co-flowing liquid–gas jets in capillary flow focusing. Phys Fluids. 2010; 22:112–105.
79. Si T, Zhang L, Li G, et al. Co-axial electrohydrodynamic atomization for multimodal imaging and image-guided therapy. Proc SPIE. 2012:8216–8221.
80. Park CH, Lee J. One step immobilization of protein encapsulated core/shell particles onto nanofibers. Macromol Mater Eng. 2010; 295(6):544–550.
81. Chen HY, Zhao Y, Jiang L. Compound-fluidic electrospray: an efficient method for the fabrication of microcapsules with multicompartment structure. Chin Sci Bull. 2009; 54(18):3147–3153.
82. Nangrejo M, Ahmad Z, Edirisinghe M. Generation of ceramic–ceramic layered composite microstructures using electrohydrodynamic co-axial flow. Ceramics International. 2010; 36(4): 1217–1223.
83. Nangrejo M, Ahmad Z, Edirisinghe M. Ceramic encapsulation with polymer via co-axial electrohydrodynamic jetting. J Microencapsul. 2010; 27(6):542–551. [PubMed: 20586700]
84. Pareta R, Edirisinghe MJ. A novel method for the preparation of biodegradable microspheres for protein drug delivery. J R Soc Interface. 2006; 3(9):573–582. [PubMed: 16849253]
85. Wu Y, Fei Z, Lee LJ, Wyslouzil BE. Coaxial electrohydrodynamic spraying of plasmid DNA/ polyethylenimine (PEI) polyplexes for enhanced nonviral gene delivery. Biotechnol Bioeng. 2010; 105(4):834–841. [PubMed: 19845020]
86. Chen H, Zhao Y, Song Y, Jiang L. One-step multicomponent encapsulation by compound-fluidic electrospray. J Am Chem Soc. 2008; 130(25):7800–7801. [PubMed: 18510318]
87. Jayasinghe SN, Townsend-Nicholson A. Stable electric-field driven cone–jetting of concentrated biosuspensions. Lab Chip. 2006; 6(8):1086–1090. [PubMed: 16874383]
88. Lastowa O, Balachandran W. Numerical simulation of electrohydrodynamic (EHD) atomization. J Electrostat. 2006; 64:850–859.

89. Enayati M, Farook U, Edirisinghe M, Stride E. Electrohydrodynamic preparation of polymeric drug-carrier particles: mapping of the process. Int J Pharm. 2011; 404(1–2):110–115. [PubMed: 21093562]

90. Li Y, Li J, Zhang H, Su Y. Microbubble suspensions prepared via electrohydrodynamic jetting process. IEEE Proc BioMed Eng and Inform. 2008; 2:445–449.

Key issues

- In comparison with existing microencapsulation/nanoencapsulation processes, coaxial electrospray offers several potential advantages such as high encapsulation rate, effective protection of bioactivity and uniform size distribution. It is especially suitable for encapsulating various drugs, proteins and bioactive agents.
- Coaxial electrospray has not been widely used for mass production of drug-loaded polymeric microparticles and polymeric nanoparticles yet. This is partially due to the multiphysical nature of the process and the complex interplays of multiple design, process and material parameters. Further development of the process requires both theoretical and experimental efforts.
- On the theoretical side, the multiphysical mechanism of coaxial electrospray has not been well studied yet. Existing numerical models are based on single-axial electrospray and cannot be directly applied to the coaxial case. Instability analysis involves multiple simplifications and assumptions, and may not reflect the actual process conditions, although the analysis results are qualitatively coincident with the experimental results. Further modeling and simulation works are necessary in order to understand the process physics, predict the process outcome and guide the process control.
- On the experimental side, most of the existing coaxial electrospray systems are custom designed by individual research laboratories without standard guidelines. To facilitate the broader application of this promising process, it is important to standardize the experimental setup for reproducibility. It is also important to carry out systematic research on design, process and material parameters that enable stable cone–jet mode and successful droplet formation. To facilitate mass production of the multilayer polymeric microparticles and polymeric nanoparticles, it is necessary to develop a nozzle array for coaxial electrospray.
- Further development and dissemination of this promising technology requires not only effective collaborations among scientific, engineering and clinical researchers, but also seamless partnership among research laboratories, biomedical engineering industry and government regulatory agencies.

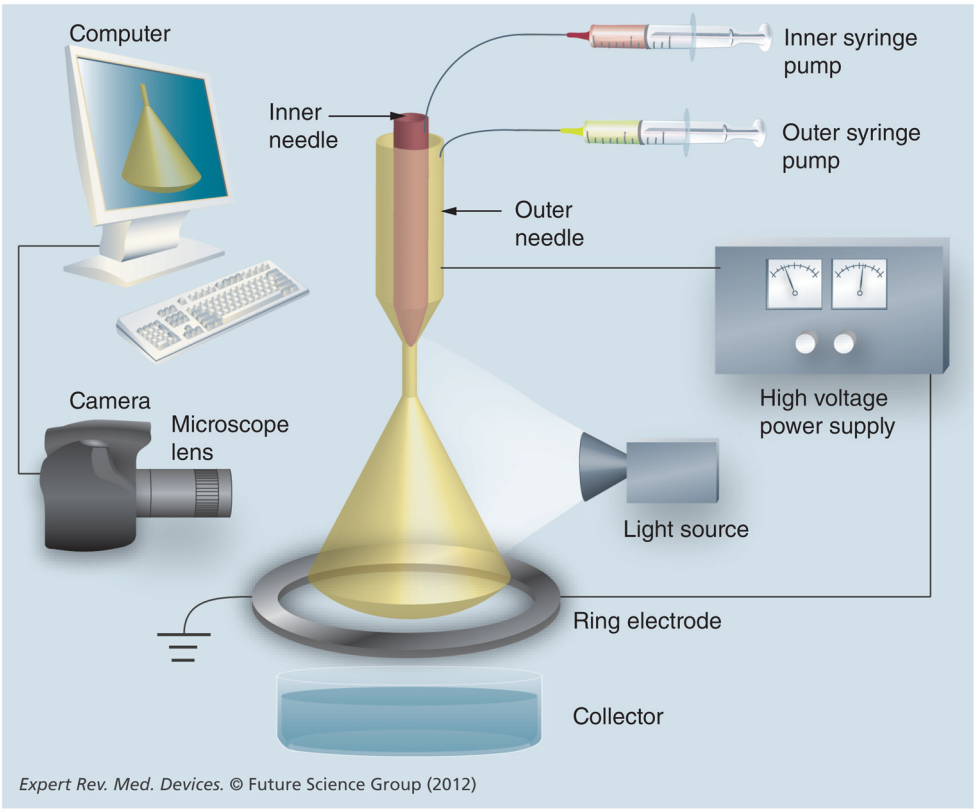

Figure 1.
Schematic setup of a typical coaxial electrospray process.

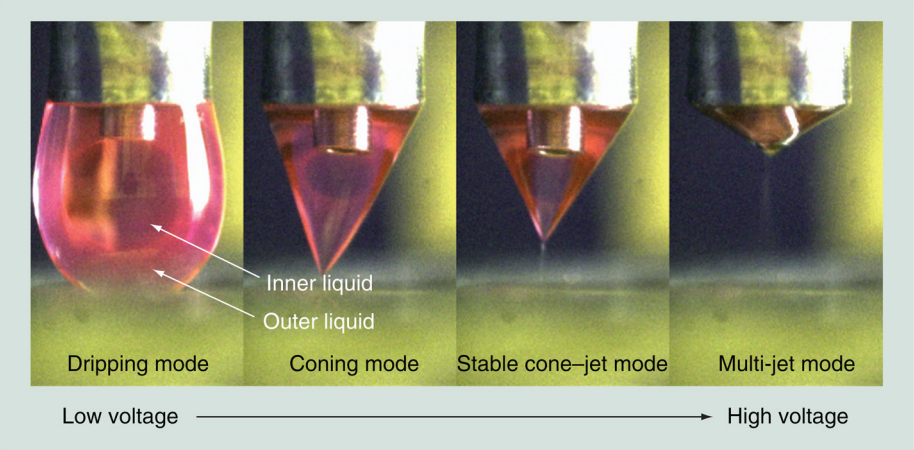

Figure 2. The mode transition in coaxial electrospray as the applied voltage increases

Reproduced from [79].

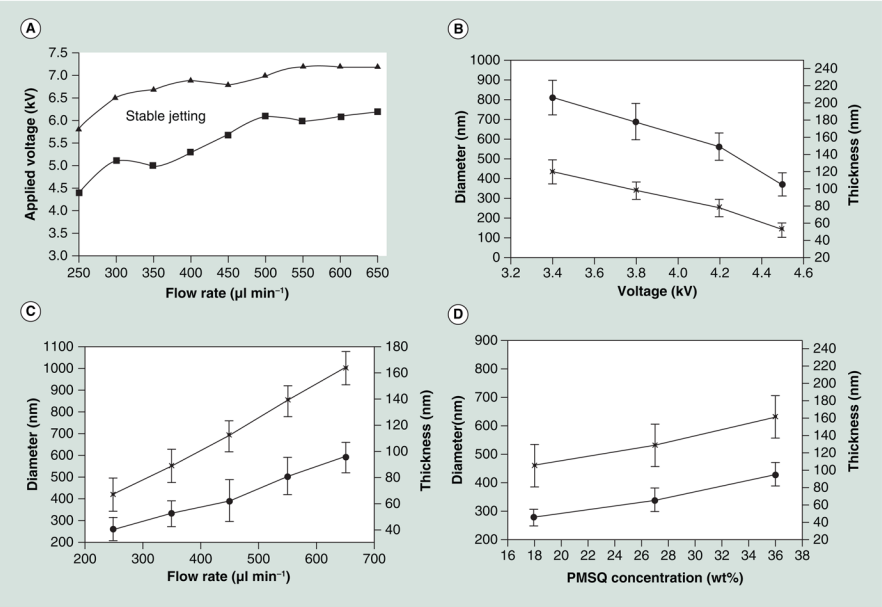

Figure 3. Correlations of the process parameters and the droplet characteristics in coaxial electrospray

(A) The working range of the applied voltages and the flow rates for a stable cone–jet flow. **(B)** Droplet diameter and thickness versus the applied voltage. **(C)** Droplet diameter and thickness versus flow rate. **(D)** Droplet diameter and thickness versus material concentration. In **(A)**, the lines with solid triangles and squares represent the upper and the lower boundaries of the stable jetting. In **(B–D)**, the lines with crosses represent droplet diameter; the lines with solid circles represent droplet thickness.

PMSQ: Polymethylsilsesquioxane.

Reproduced with permission from [68].

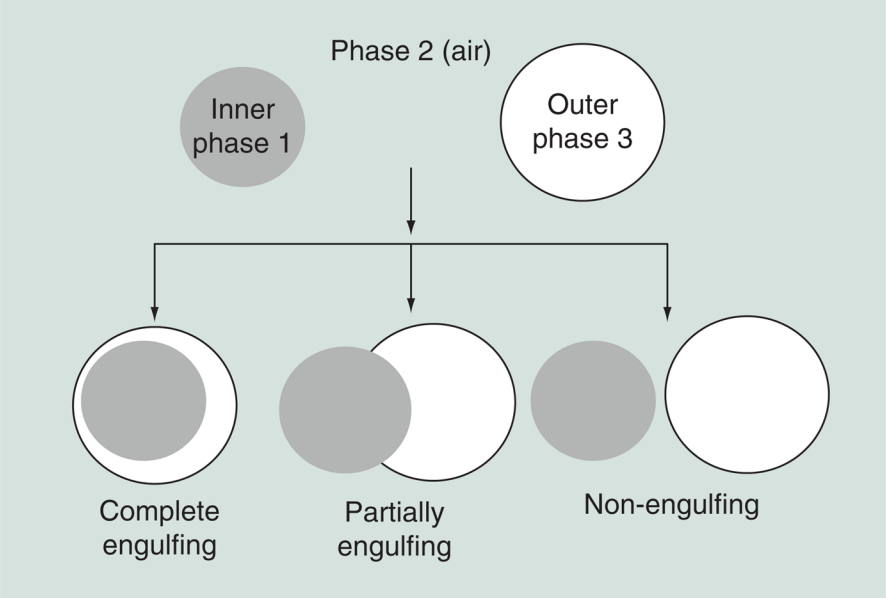

Figure 4. Three possible engulfing conditions as the inner phase 1 and outer phase 3 brought into contact with phase 2 in a coaxial electrospray process
Reproduced with permission from [54].

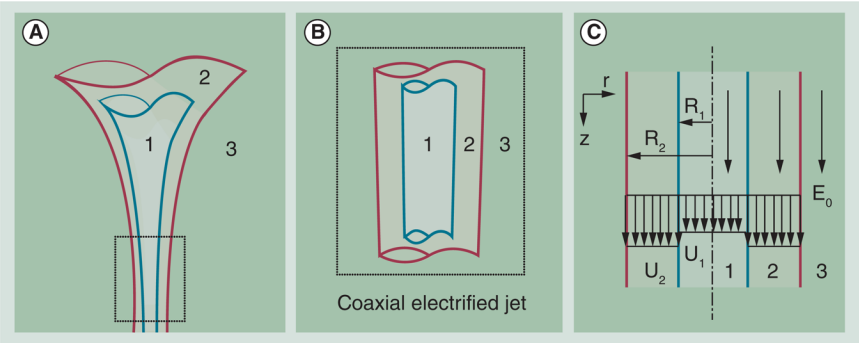

Figure 5. Schematic descriptions of (A)
the coaxial cone–jet configuration; **(B)** the coaxial electrified jet; **(C)** the simplified theoretical model.
1: the inner liquid; 2: the outer liquid; 3: the ambient gas.

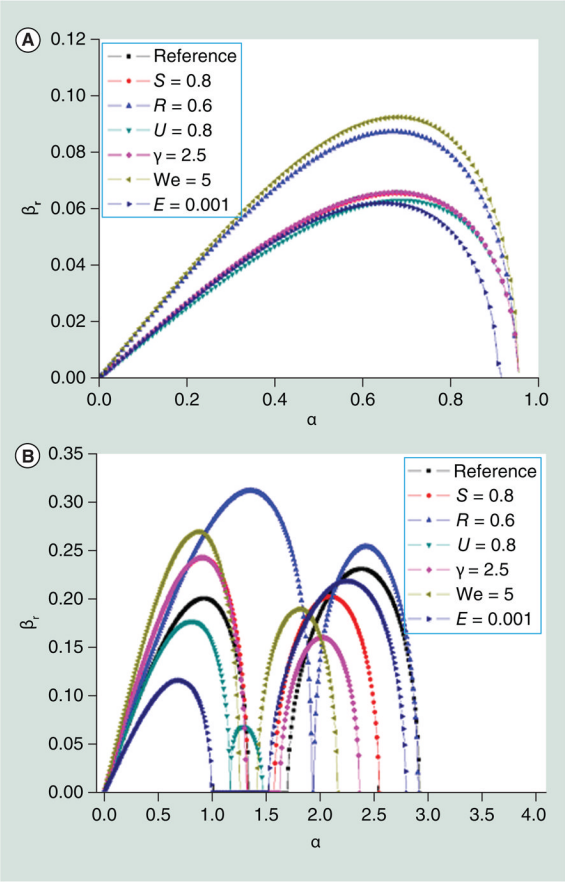

Figure 6. Effects of the parameters on the growth rate βr of the paravaricose mode (A) and the parasinuous (left) and transitional (right) modes (B)

'Reference' indicates the referenced dimensionless parameters We = 10, E = 10^{-4}, Q = 10^{-3}, S = 1.2, R = 0.8, U = 0.4, γ = 1.5, ε_{1p} = 60, ε_{2p} = 20, K = 10, n = 0 and the others are obtained by changing only one parameter in 'Reference'.

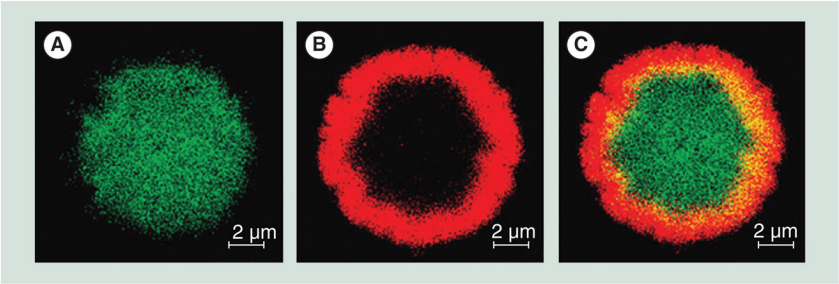

Figure 7. Structure of the fabricated microspheres

FITC-labeled BSA was added into the protein solution, and rhodamine-B was loaded into the PLGA solution before fabrication. The resulting microsphere shows a core-shell structure **(C)** with PLGA as the shell **(B)** and protein solution **(A)** as the core and PLGA as the shell **(B)**.

BSA: Bovine serum albumin; FITC: Fluorescein isothiocyanate;
PLGA: Poly(lactic-co-glycolic acid).

Reproduced with permission from [62].

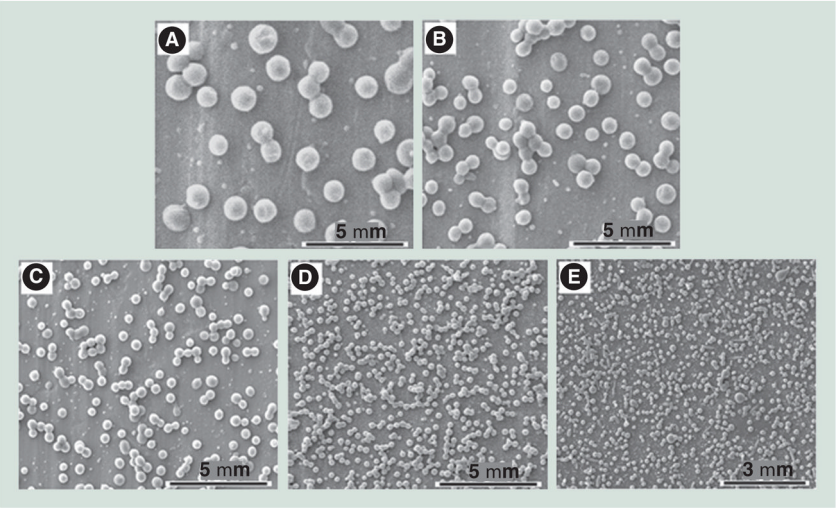

Figure 8. Budesonide-loaded PLGA particles produced by tuning the concentration and conductivity of PLGA solution

(A) 5 wt.% (1200 nm), **(B)** 3 wt.% (800 nm), **(C)** 0.5 wt.% (400 nm), **(D)** 0.2 wt.% (289 nm) and **(E)** 0.5 wt.% (with 10 mM KCl, 165 nm) while the flow rate for the outer liquid was held constant at 5 μl/min.

PLGA: Poly(lactic-co-glycolic acid).

Reproduced with permission from [17].

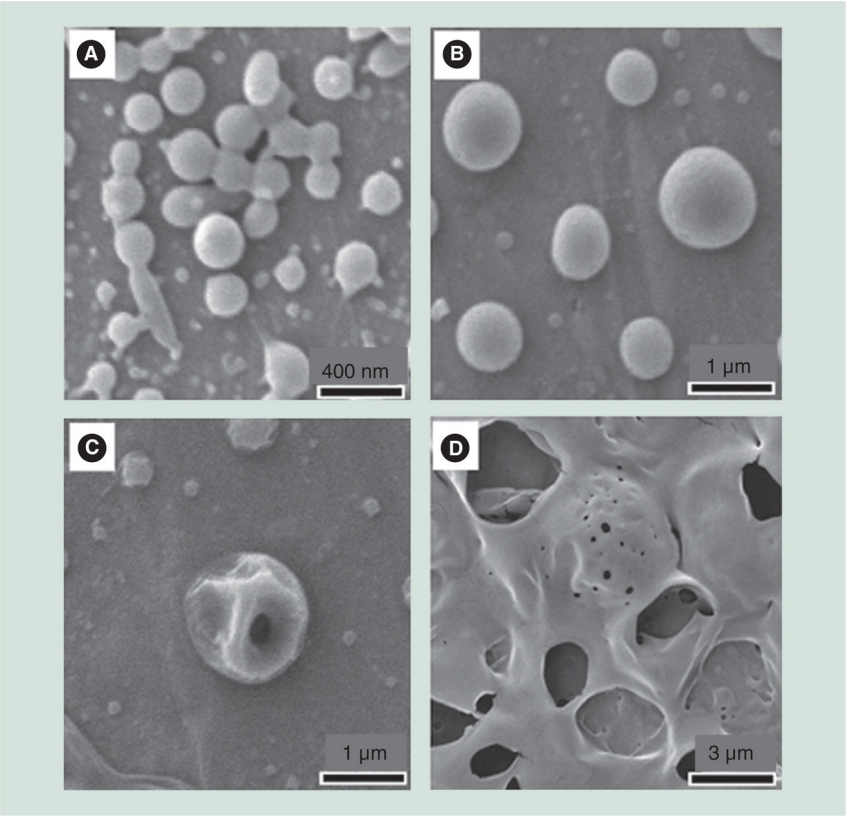

Figure 9. The morphology change of 165 nm budesonide-loaded poly(lactide-coglycolide) (PLGA) particles produced by coaxial electrospray at different release times: (A) at initial, (B) after 15 min releasing, (C) after 25 min releasing and (D) after 24 h releasing
Reproduced with permission from [17].

Table 1

Different configurations for coaxial electrospray.

Study (year)	Inner needle size (μm)	Outer needle size (μm)	Inner flow rate (ml/h)	Outer flow rate (ml/h)	Applied voltage (kV)	Electrode distance†	Inner and outer needle height	Ref.
Lopez-Herrera *et al.* (2003)	500 ID 900 OD	1100 ID 1500 OD	0.3	12	7.5	25 mm	Same	[51]
Chen *et al.* (2005)	200 ID 550 OD	700 ID 1200 OD	0.75	0.5	6	20 mm	Same	[67]
Mei *et al.* (2008)	127 ID 508 OD	762 ID 1270 OD	0.06	0.06	>4.5	NA	Same	[54]
Chang *et al.* (2010)	150 ID 300 OD	685 ID 1100 OD	9	18	4.2	12 mm	Inner raised by 2 mm	[41]
Farook *et al.* (2007)	150 ID 300 OD	685 ID 1100 OD	18	18	8.7	12 mm	Inner raised by 2 mm	[38]
Park *et al.* (2007)	2032 ID 3175 OD	4064 ID 6350 OD	6	12	14.5–16.5	10 mm	Inner descended by 0.5 mm	[60]
Xie *et al.* (2008)	394 ID 720 OD	2000 ID 3000 OD	0.2	5	8.5–15.5	NA	Same	[23]

†Electrode distance refers to the distance between the tip of the nozzle to the horizontal plane of the ground electrode.

ID: Inner diameter; NA: Not available; OD: Outer diameter.

Table 2

Summary of material combinations and process outcomes for coaxial electrospray.

Study (year)	Shell material	Core material	Size	Collection method	Inner or outer driving	Main features of the referred article	Ref.
Ahmad *et al.* (2008)	From inside to out: air, glycerol/polyethylene oxide, olive oil		~50 μm	Unspecified	Unspecified	Three-layer droplet	[49]
	From inside to out: BSA, starch, polyurethane		~200 nm	Methanol/ice water			
Bocanegra *et al.* (2005)	Cocoa butter	Water; oil & water emulsion	~10 μm	Cooling pipe with vacuum pump	Inner	Particle delivering food ingredients; size vs flow rate	[63]
Chang *et al.* (2010; 2010)	PMSQ (in ethanol)	Perfluorohexane	0.3–1 μm	Distilled water	Outer	Hollow polymer microspheres; shell thickness and size vs concentration, voltage, flow rate	[41,68]
Chen *et al.* (2008; 2009)	Somos liquid $Ti(OBu)_4$ solution	Glycerol paraffin oil	~20 μm 1~10 μm	Aluminum foil/glass plate	Outer	Particles with 2~4 inner compartments	[81,86]
Chen *et al.* (2005)	Ethanol, glycerol, Tween 80	Cooking oil	5~10 μm	Glass plate with a oil layer	Outer	Spray modes vs flow rates, voltage	[67]
Enayati *et al.* (2010; 2011)	PLGA (in DMAC)	Estradiol in methanol	0.1~4 μm	Simulated body fluid/ethanol	Unspecified	Release study of drug-encapsulated particles	[24,89]
	PMSQ (in ethanol)	Air	0.1~1 μm	Distilled water	Outer	Size vs flow rate	
Farook *et al.* (2009; 2007; 2008; 2009; 2009; 2007)	Glycerol	Air	2–10 μm	Glycerol	Outer	Spray modes versus flow rates, voltage size vs flow rate	[22,38–40,42,43]
	PMSQ (in ethanol)	Air	4~8 μm	Distilled water	Outer	NA	
	Phospholipid, Tween 80	Air	~10 μm	Glycerol	Outer	Effect of Tween 80 as surfactant on particle size, stability and so on	
	Glycerol, Tween80/Zirconia	Air	10~50 μm	Glycerol	Outer	NA	
	Lipid	Air	1~10 μm	Distilled water	Outer	Size vs flow rate, temperature	

Study (year)	Shell material	Core material	Size	Collection method	Inner or outer driving	Main features of the referred article	Ref.
Hwang *et al.* (2008)	PCL (in chloroform)	PS/PMMA (in chloroform)	2–6 μm	Unspecified	Unspecified	A special system: inner liquid forms shell of particle, while outer liquid forms core	[37]
Jayasinghe *et al.* (2006)	Medical grade PDMS oil	Living cells + medium	30 μm	Sterile dish containing cell culture medium and antibiotic	Unspecified	Particles encapsulating living cells	[87]
Jing *et al.* (2011)	TiO_2 (in Ethanol)	Paclitaxel, Fe_3O_4, quantum dots (in olive oil)	1~3 μm	Unspecified	Unspecified	Multifunctional agent for fluorescence and magnetic imaging and drug delivery	[71]
Kim *et al.* (2010)	From inside to out: EG, olive oil and 4-HBA		10~20 μm	Oil film with a 4-HBA layer	Inner	Particles with three concentric layers	[50]
Lee *et al.* (2010)	PLGA (in acetonitrile)	Budesonide/EGCG (in acetonitrile)	0.2~1 μm	Water	Outer	Release study of drug-encapsulated particles; size vs concentration	[17]
	From inside to out: PSS, PLGA, PSS (in acetonitrile)		2~5 μm	Olive oil	Outer	Particles with three concentric layers; release study of drug- encapsulated particles	
	From in to out: EGCG, Budesonide, PLGA (in acetonitrile)		2~5 μm	Aluminum foil			
Li *et al.* (2008)	Glycerol, PEG400	Air	10 μm	Glycerol	Outer	Effect of PEG400 on bubble lifetime	[90]
Loscertales et al. (2002); Lopez-Herrera *et al.* (2003)	Somos liquid	EG	20~50 μm	Unspecified	Outer	Introduction of driving force concept and scaling laws for electric current and particle size	[21,51]
	Somos liquid	EG, additive			Inner		
	Olive oil	Water			Inner		
Loscertales *et al.* (2002)	Olive oil	Water	0.1~10 μm	Water plate	Inner	First publication for coaxial electrospray	[21]
	Somos liquid	EG			Outer		
Mei *et al.* (2007; 2008)	Olive oil, mineral oil	Ethanol, tributyl phosphate, ethylene glycol, and triethylene glycol	1~10 μm	ELPI impaction stage	Inner	Introduction of concepts charge relaxation lengths	[53,54]

Study (year)	Shell material	Core material	Size	Collection method	Inner or outer driving	Main features of the referred article	Ref.
						and inertial breakup lengths	
Nangrejo *et al.* (2008)	Zirconia (in olive oil)	Alumina (in glycerol)	~30 μm	Quartz slide	Inner	Particles with ceramic core and shell; spray modes vs flow rates, voltage	[82,83]
	Alumina (in glycerol)	Zirconia (in olive oil)			Outer		
	PMSQ (in ethanol)	Alumina (in glycerol)	1~40 μm	Water	Unspecified	Particles with polymer shell and ceramic core; spray modes vs flow rates, voltage	
Nie *et al.* (2010)	Suramin, PLGA	Paclitaxel, PLLA	5~20 μm	Ethanol	Unspecified	Animal study of drug delivery by particles fabricated using electrospray	[45]
	Paclitaxel, PLGA	Suramin, PLLA					
Pancholi *et al.* (2008)	Phospholipid	Air	3~500 μm	Glass slide	Outer	Size vs flow rate/ voltage	[39]
Pareta *et al.* (2006)	PDMS	BSA, starch (in DMSO)	5–6 μm	Acetone with PDMS	Inner	Release study of drug-encapsulated particles	[84]
Park *et al.* (2010)	PLGA (benzaldehyde/ethylacetate)	Lysozyme/polyvinylpyrrolidone (in water)	1 μm	Unspecified	Inner	Particles were attached to nanofibers	[80]
Park *et al.* (2011)	Olive oil	Ethanol	10~60 μm	Stainless steel mesh ground plate	Inner	Fabricate MPs using multijet mode	[60]
Park *et al.* (2011)	Chitosan	Fucoidan	5~9 μm	Surface of metal plates	Unspecified	Combined coaxial electrospray with spray drying	[47]
Wang *et al.* (2009)	PLGA (in dichloromethane)	BSA, IGF, gelatin (in water)	5 μm	Aluminum foil	Inner	Release study of drug-encapsulated particles	[62]
Wu *et al.* (2009; 2010)	Lipoplex (in ethanol)	G3139 (in PBS, oblimersen sodium)	200 nm	Aluminum dish containing PBS	Unspecified	Release study of drug-encapsulated particles; size vs	[61,85]
	pDNA (in OPTI-MEM solution)	PEI (in OPTI-MEM solution)	0.5–1 μm	Aluminum dish containing PBS	Unspecified		

Study (year)	Shell material	Core material	Size	Collection method	Inner or outer driving	Main features of the referred article	Ref.
						concentration, flow rate	
Xie *et al.* (2008)	PLGA (in dichloromethane)	Bovine serum albumin or lysozyme	5~10 μm	Aluminum foil	Inner	Release study of drug-encapsulated particles	[23]
Xu *et al.* (2008)	PLA (in dichloroethane)	BSA (in water)	~5 μm	Unspecified collector	Inner	Size vs concentration, flow rate and voltage	[44]

4-HBA: 4-Hydroxylbutyl acrylate; BSA: Bovine serum albumin; DMSO: Dimethylsulfoxide; EG: Ethylene glycol; NA: Not available; PCL: Polycaprolactone; PDMS: Polydimethylsiloxane; PEI: Polyethylenimine; PLGA: Poly(lactide-coglycolide); PLLA: Poly-L-lactic acid; PMMA: Poly(methyl methacrylate); PMSQ: Polymethylsilsesquioxane; PS: Polystyrene.